The Deposition of Silicon Films by Pyrolytic Decomposition of SiF_2 Gas

M. Janai, S. Aftergood, R. B. Weil, and B. Pratt

Department of Physics and Solid State Institute, Technion-Israel Institute of Technology, Haifa 32000, Israel

ABSTRACT

Production of silicon films by a silicon fluoride transport reaction is described here. The effect of various deposition parameters including temperature, partial pressure, and gas flow rate on the deposition kinetics was investigated. X-ray analysis, surface electron spectroscopy, optical absorbance and reflectance, and electrical measurements indicate that the films have properties similar to those of silicon films obtained by CVD from silane.

The silicon fluoride transport reaction has been suggested by Wolf *et al.* as a low cost purification process of metallurgical-grade silicon. Combined with a simultaneous on-line CVD process the method can be used for the production of silicon sheets for photovoltaic solar cell arrays (1, 2). The purification capability of this process has been further investigated by Ingle *et al.* (3). The process makes use of the cyclic reaction sequence

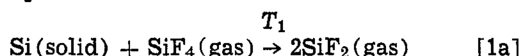

$$Si(solid) + SiF_4(gas) \xrightarrow{T_1} 2SiF_2(gas) \quad [1a]$$

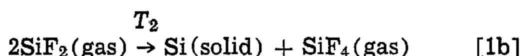

$$2SiF_2(gas) \xrightarrow{T_2} Si(solid) + SiF_4(gas) \quad [1b]$$

T_1 is a temperature above 1100°C and T_2 is in the range of 450°-850°C. In a complete cycle of the process the SiF_4 gas reacts with silicon at temperature T_1 to yield SiF_2, which in turn decomposes on a substrate held at temperature T_2, resulting in the deposition of a solid silicon film and the release of SiF_4 gas. The SiF_4 is circulated in the system in a closed loop. The purification potential of the process results from the preferential reaction of SiF_4 with the silicon rather than with its impurities at the temperature T_1, and from the higher condensation temperature of the metalfluoride impurities which may be formed in the high temperature zone (1-3).

We have studied the above transport reaction for its thin film deposition capability, with pure solid silicon as the starting material. This process may be useful in polysilicon deposition for microelectronics purposes since deposition takes place even at the relatively low temperature of 550°C and the films have high specular reflectance, which is desirable for photolithographic processing. Films deposited at 550°C, however, are amorphous and for some applications might have to be annealed at a higher temperature for a short period of time to increase the charge carrier mobility. A further advantage of the CVD process utilizing the silicon fluoride transport reaction is that oxygen leaking into the system may be easily adsorbed on an appropriate getter, as discussed below. In the silicon fluoride transport process the SiF_4 may be cycled again and again through the deposition in cost savings.

We have reported previously (5) on a deposition system where SiF_2 is transported from the high temperature zone to the substrate without going through an intermediate zone with a temperature lower than that of the substrate. In the present work we have studied a deposition system where the gas is quenched down to room temperature at the exit of the high temperature zone (T_1) and is transported at room temperature to the substrate, which is held at temperature T_2. The effect of various deposition parameters on the deposition kinetics and the properties of the resultant film are described below.

Key words: thin films, amorphous Si:F, polymerization, CVD kinetics.

System Description

The deposition system is schematically depicted in Fig. 1. About 200 silicon cubes 2.5 mm on edge each were cut from a Czochralski grown silicon single crystal. The cubes were held in a vertical quartz tube which was mounted in a resistively heated furnace. The temperature of the silicon (T_1) was monitored by an external thermocouple. The temperature of the silicon cubes was between 0° and 20°C higher than the reading of the external thermocouple, depending on the height level of the silicon in the column. The walls of the tube at the exit of the furnace were cooled, forming a temperature gradient of approximately 200°C/cm between 1000° and 100°C in the gas.

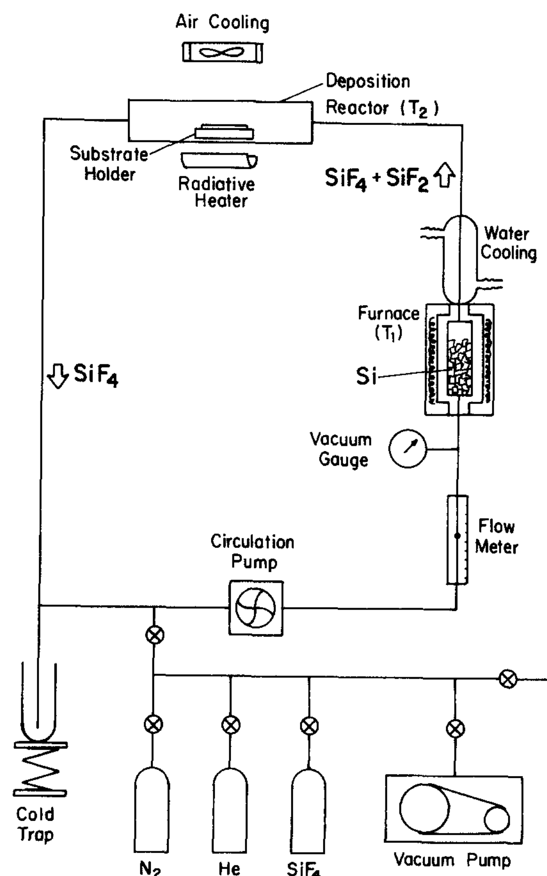

Fig. 1. Schematic illustration of the deposition system

Downloaded on 2015-06-07 to IP 128.210.126.199 address. Redistribution subject to ECS terms of use (see ecsdl.org/site/terms_use) unless CC License in place (see abstract).

The gas was transported from the high temperature zone to the deposition zone in a 70 cm long glass tube. The substrates in the deposition zone were supported on a radiatively heated graphite holder, placed in a horizontal quartz tube 45 mm in diameter. The walls of the deposition reactor were air-cooled. The temperature gradient over the deposition region was less than 1°C/cm. A Dia-Vac™ pump was used to circulate the gas in the system. A Matheson Model 603 ball type flowmeter monitored the gas flow rate. The total volume of the system was approximately 1.5 liters.

In a typical deposition cycle the silicon cubes were rinsed in HF acid to remove any oxide layer. The silicon cubes were placed in the quartz tube and the system was pumped, purged with nitrogen and helium, and again pumped down to a vacuum of 0.05 Torr. The pump was turned off and SiF_4 from an external tank was admitted into the system until the desired SiF_4 initial pressure was achieved. The SiF_4 was then solidified in a liquid-air trap inside the system. Once the SiF_4 completely solidified the heaters were turned on and the system was pumped again to remove any volatile species. Once the temperatures T_1 and T_2 had stabilized the vacuum pump was disconnected, the SiF_4 was re-evaporated into the system, and the circulation pump was turned on. The pressure in the hot system was usually 7% higher than the SiF_4 initial pressure of the room temperature system. In a typical deposition cycle (*e.g.*, sample E-14) we used the following deposition parameters: SiF_4 initial pressure = 80 Torr, T_1 = 1100°C, T_2 = 600°C, and flow rate 0.3 mol/hr. No carrier gas was used. Unless otherwise specified, each deposition run lasted 30 min. At the end of each deposition run the SiF_4 gas was returned to the storage tank by refreezing it. The SiF_4 pressure in the system and the silicon weight were determined before and after the deposition.

Fused silica substrates were used in most depositions. The gas source was Matheson 99.7% purity SiF_4 (6). As indicated above, the gas was further purified by freezing it to 77 K and pumping off the volatile species.

Effect of Deposition Parameters on Deposition Kinetics

Experimental.—The thickness of the films was routinely determined from their reflectance traces in an infrared spectrophotometer by the interference fringes method (7). For the calibration of these measurements we determined first the wavelength dependence of the refractive index, $n(\lambda)$, of one of our samples whose thickness was determined with an interference microscope. This refractive index was used in turn to calculate the thickness of all other samples according to

$$d = \frac{N \cdot \lambda_N}{2n(\lambda_N)} \qquad (N = 1,2,\ldots)$$

where d is the film thickness, N is the order of the reflectance minima, and λ_N is the wavelength of the minima of order N.

Thickness uniformity.—The uniformity of the film thickness was found to depend mostly on the method of cooling the walls of the deposition reactor, probably due to its effect on convection currents in the gas. Under usual deposition conditions the film thickness uniformity was better than 1%/cm perpendicular to the gas flow direction, and monotonically decreasing at about 4%/cm over an 8 cm long sample parallel to the gas flow direction. The latter effect was probably associated with the depletion of SiF_2 from the gas along the direction of flow. In the experiments reported below we used 1 cm² samples placed reproducibly on the substrate holder about 3 cm from its leading edge.

Time dependence of film thickness.—Figure 2 shows the dependence of the sample thickness on the deposition time for periods between 20 and 60 min. The linear curve which passes through the origin indicates that the deposition rate is constant with time. It implies that any time-dependent variables in the deposition system (such as the SiF_2 and SiF_4 partial pressures) either reach their steady-state values quickly relative to our deposition time scale, or their time-dependent effect on the variation of the deposition rate is negligible.

Reaction temperature (T_1).—The temperature T_1 was varied between 1060° and 1200°C. Figure 3 shows a semilog plot of the film thickness deposited in 30 min *vs.* the reciprocal of temperature T_1. For temperatures lower than 1060°C the deposited layer was too thin to be measured by our optical technique. We did not exceed 1200°C because of material limitations imposed by the quartz tube. As shown below, the deposition rate is proportional to the SiF_2 generation rate, so that Fig. 3 indicates a generation rate activation energy of 54 ± 4 kcal/mol (2.3 ± 0.2 eV).

Deposition temperature (T_2).—The temperature T_2 was varied between 475° and 675°C. Figure 4 shows a semilog plot of the 30 min deposition thickness *vs.* reciprocal substrate temperature. Below 550°C the deposition rate increased with temperature with an ac-

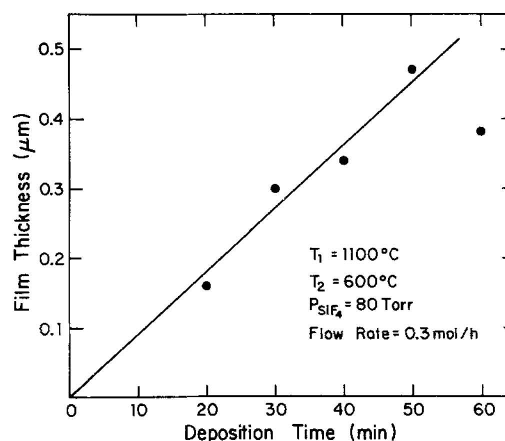

Fig. 2. Dependence of the deposited silicon film thickness on the deposition time.

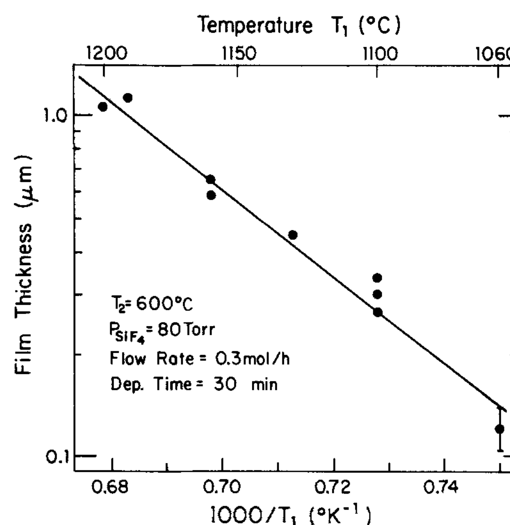

Fig. 3. Dependence of the deposition rate on the temperature of the reactor in which SiF_2 is formed.

Downloaded on 2015-06-07 to IP 128.210.126.199 address. Redistribution subject to ECS terms of use (see ecsdl.org/site/terms_use) unless CC License in place (see abstract).

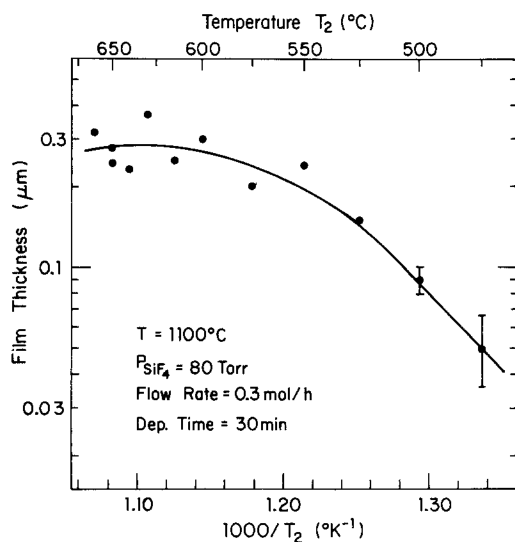

Fig. 4. Dependence of the deposition rate on the substrate temperature.

tivation energy of 29.0 ± 1.5 kcal/mol (1.26 eV). The maximum deposition rate was achieved around a substrate temperature of 620°C, and was almost constant over the temperature range 600°-675°C. Depositions made with a different setup (5) indicated that above 675°C the deposition rate decreases with temperature, and above 900°C no silicon deposition could be detected even after extended deposition periods.

Flow rate.—The gas flow rate (measured in units of moles per unit time) was determined from a calibration curve of the 603 flowmeter for SiF_4 under standard conditions (760 Torr, 21°C) by multiplying the standard flow rate by $(P/760)^{1/2}$ where P is the system pressure in Torr. As shown below, under most deposition conditions the molar fraction of SiF_2 in the system was small, particularly in the section of the system following the deposition reactor. Since the flowmeter was mounted after the deposition reactor the monitored flow was practically that of the SiF_4 alone. Figure 5 shows the dependence of the deposition rate on the gas flow rate for flow values between 0.18 and 0.63 mol/hr. As seen from the figure, in this range the deposition rate increases linearly with flow rate.

Pressure.—Since the molar fraction of SiF_2 in the system was relatively low the total pressure of the system was approximately the partial pressure of the SiF_4 gas. Depositions were made with SiF_4 initial pressures between 70 and 220 Torr. In these experiments we kept the setting of the ball of the flowmeter at a constant height for all pressures. Under these conditions (8)

$$\rho\nu^2 = \text{constant} \quad [2]$$

where ρ is the density of the gas in the system in units of mass per unit volume (or moles SiF_4 per unit volume) and ν is the gas flow velocity in units of volume per unit time. From Eq. [2] we obtain that

$$\nu = A \cdot \rho^{-1/2} \simeq A \cdot 135 \cdot P^{-1/2} \quad [3]$$

and

$$\text{flow rate} = \nu \cdot \rho \simeq A \cdot P^{1/2}/135 \quad [4]$$

where P is the initial pressure in Torr in the room temperature system, ρ,ν, and the flow rate are given in units of mol/liter, liters/hr, and mol/hr, respectively, and A is a system constant obtained experimentally by multiplying ν by $\rho^{1/2}$, and it depends on the setting of the flowmeter. The constant 135 is the square root of the standard pressure (760 Torr) times the specific volume of SiF_4 at room temperature at 760 Torr (24.08 liter/mol) (6). Under the condition of Eq. [2], we observed no difference in deposition rate for the various SiF_4 initial pressures. For $A^2 = 21$ mol · liter/hr^2, we obtained a deposition rate of 0.32 ± 0.03 μm per 30 min deposition or 1.8 ± 0.2 Å/sec (see Fig. 6, left scale).

During depositions, which all started with given initial SiF_4 pressures, a pressure drop varying between 5 and 40% was observed. This pressure drop was nearly linear with deposition rate with varying T_1. The pressure drop ΔP for experiments with various initial SiF_4 pressures, at constant T_1 and $\rho\nu^2$, is shown in Fig. 6 (right scale). From the slope in Fig. 6 and the deposition parameters given in the figure one gets a pressure drop $\Delta P/P = 12\%$. It can be seen that the absolute pressure drop was linear with the initial pressure, for a constant $\rho\nu^2$ value, while under the same conditions the deposited film thickness was independent of the pressure. (The scatter of the experimental results probably reflects the degree of control we had on the parameter $A^2 = \rho\nu^2$ and on the system temperatures in the various depositions.) From the above considerations we obtain the empirical relation

$$\Delta P/P = B(T) \cdot f(\rho\nu^2) \cdot \Delta t \quad [5]$$

where B is a constant depending on the system temperatures, Δt is the deposition time, and f is a function of the parameter $\rho\nu^2$, determined by the kinetics of the

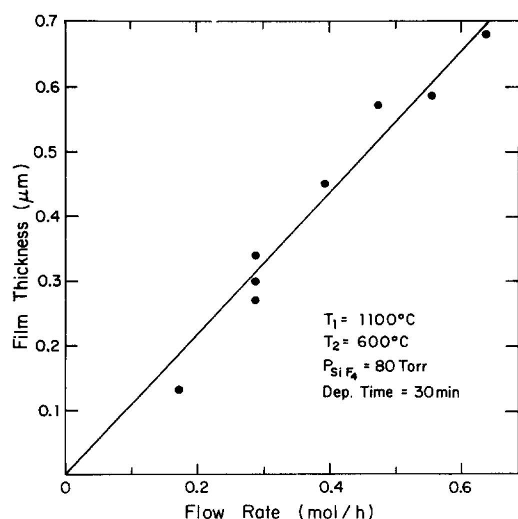

Fig. 5. Dependence of the deposition rate on the SiF_4 gas flow rate for a constant pressure of SiF_4 in the system.

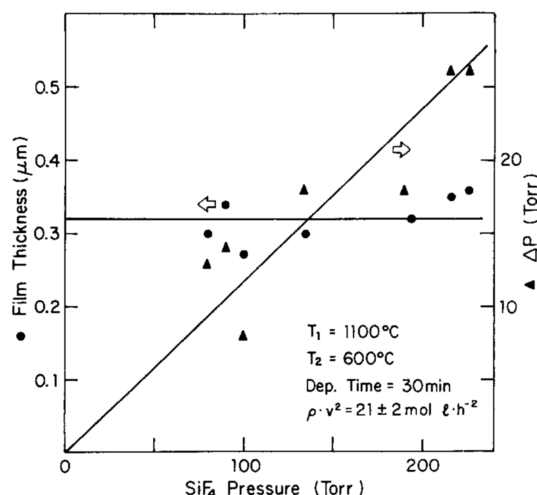

Fig. 6. Dependence of the deposition rate (●, left scale) and the pressure drop in the system during a 30 min deposition (▲, right scale) as a function of the initial pressure in the system.

Downloaded on 2015-06-07 to IP 128.210.126.199 address. Redistribution subject to ECS terms of use (see ecsdl.org/site/terms_use) unless CC License in place (see abstract).

mechanism causing the pressure drop. From measurements of ΔP under constant initial P and varying flow rates we obtained $\Delta P \propto \nu^{1.8 \pm 0.3}$ which suggests that in Eq. 5, $f(\rho\nu^2) = \rho\nu^2$. The probable reason for the pressure drop has been identified as condensation of SiF_2 molecules in the form of $(SiF_x)_n$ polymers on the water-cooled walls of the tube following the high temperature zone (9). In Table I the results of two similar deposition runs—one with, and one without water-cooled walls—are given. The original reason for water cooling the walls at the exit of the high temperature zone was to reduce the length of the tube section over which the wall temperature was between 450° and 900°C, thus limiting the back-reaction given by Eq. [1b] in the unwanted sections of the system. The results shown in Table I demonstrate, however, that with no water cooling, where the tube walls were heated to 100° ~300°C by the hot gas flow, polymerization was significantly reduced and the deposition rate was increased. As seen from the table, without water cooling the percentage pressure drop was reduced by a factor of 4, and the deposition rate was increased by a factor of 1.8. The pressure drop in depositions E-44 and E-45 implies a loss of 11×10^{-4} and 2.5×10^{-4} mol of SiF_4 from the gas, respectively. Assuming (9) that the majority of the polymerization is of the form $(SiF_2)_n$, this SiF_4 gas loss is equivalent to the removal of an equal number of mols of silicon transported from the high temperature zone, *i.e.*, 31 and 7.7 mg silicon, respectively. The loss of the transported silicon due to polymerization is significant in view of the fact that the total silicon weight deposited on the substrate and substrate holder in these two depositions was only 6.8 and 12.4 mg, respectively.

Other observations.—A direct correlation between the total silicon mass tranport, as measured by the loss of silicon weight in the high temperature reaction zone during a deposition, and the thickness of the deposited film was observed. The weight loss in a typical deposition run (*e.g.*, in deposition E-14) was 120 mg. However, only approximately 3% of the transported silicon coated the substrate and substrate holder in that deposition experiment. From the observed value of ΔP we know that 13% of the transported silicon was lost in condensation of $(SiF_2)_n$ polymers. The rest of the transported silicon appeared as deposits on the walls of the tube at the exit of the high temperature zone where the temperature was in the range of 450°-900°C. Silicon deposits were observed also on the walls of the deposition reactor. A thin silicon deposit was also observed on the hot wall at the entrance to the high temperature reactor, probably due to SiF_2 which did not decompose in the deposition zone and so completed a full cycle in the system. This happened particularly with low substrate temperature depositions. A full flow cycle in the system at F.R. = 0.3 mol/hr took 1.25 min, which sets a lower limit on the lifetime of the SiF_2 molecule in the gas.

The diffuse part of the reflectance of the films deposited below T_2 = 700°C was equal to or lower than that of silicon films deposited from silane. During deposition, under intense illumination of the gas

Table I. Summary of results of two similar depositions, one with water cooling of the walls of the glass tube at the exit of the high temperature reaction zone, and the other without water cooling.

Deposition parameters / Deposition results	T_1 = 1160°C, T_2 = 600°C, P = 80 Torr F.R. = 0.3 mol/hr; dep. time = 30 min. With water cooling	Without water cooling
Sample No.	E − 44	E − 45
Deposited film thickness	0.58 μm	1.05 μm
Pressure drop	17%	4.3%
Source silicon weight loss	293 mg	335 mg

white smoke could be observed, probably arising from $(SiF_2)_n$ long polymer chains swept along by the gas stream. This smoke was minimized by water cooling the tube between the high temperature reactor and the deposition reactor. However, the presence of this smoke did not affect the smoothness of the deposited silicon films. In fact, the smoothness of the films was so high that it was difficult to focus the beam of a scanning electron microscope on the sample surface because of lack of features.

After some depositions, a thin oxide layer could be observed on the silicon cubes at the bottom of the silicon column in the high temperature reactor. By weighing the silicon at the end of each deposition run before and after rinsing it in HF acid we estimate a a typical oxidation rate of 2 mg SiO_2 per deposition cycle, which is equivalent to an oxygen leak of 4.5×10^{-5} mol per deposition cycle. No other effects of this oxygen leak (or outgassing) could be observed in the system and in particular no oxygen was observed in the deposited films. In view of the fact that there was no outlet for this gas during the deposition we conclude that the lower section of the silicon column in the flow system acts as a getter to remove oxygen from the circulating gas.

Discussion of Deposition Kinetics Experimental Results

Our results for depositions at $T_2 > 550$°C are consistent with the assumption that the rate-limiting process of the transport reaction is the conversion of SiF_4 into SiF_2 in the high temperature zone (2). In the high temperature reaction zone equilibrium conditions prevail and the reaction there can be written as

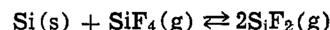

$$Si(s) + SiF_4(g) \rightleftarrows 2SiF_2(g)$$

$Kp(T)$, the pressure equilibrium constant of the reaction, is given by

$$Kp(T) = P_{SiF_2}{}^2/P_{SiF_4} \quad [6]$$

where P_{SiF_2} and P_{SiF_4} are the partial pressures of the SiF_2 and SiF_4 gases, respectively. Out of each mol of SiF_4 entering the high temperature reaction zone, a fraction α is converted into pairs of SiF_2 molecules. The partial pressures in the high temperature reactor can be written as

$$P_{SiF_4} = [(1-\alpha)/(1+\alpha)] \cdot P \quad [7a]$$

and

$$P_{SiF_2} = [2\alpha/(1+\alpha)] \cdot P \quad [7b]$$

where P is the sum of the partial pressures $P_{SiF_4} + P_{SiF_2}$. In terms of α, the pressure equilibrium constant can be written as

$$Kp(T) = 4\alpha^2 P/(1-\alpha^2) \quad [8]$$

which for small values of α gives

$$\alpha \cong (Kp(T)/4P)^{1/2} \quad [9]$$

The experimental value of α can be obtained by dividing the total number of transported silicon mols per deposition run by the total number of SiF_4 mols that flowed through the reactor. Equation [9] predicts that under equilibrium conditions in the high temperature reactor α will be proportional to the inverse square root of P, and will be temperature activated with half the activation energy of $Kp(T)$. Fitting the results of our weight-loss measurements to the functional dependence given by Eq. [9] we obtain

$$\alpha = [1.15 \times 10^8/P^{1/2}] \cdot \exp(-E/RT_1) \quad [10]$$

where $E = 54 \pm 4$ kcal/mol, $R = 1.987 \times 10^{-3}$ kcal/mol · K, T_1 is the temperature in K, and P is given in Torr. The highest value of α in our experimental regime, $\alpha \simeq 0.13$, was obtained for T_1 = 1473 K and

Downloaded on 2015-06-07 to IP 128.210.126.199 address. Redistribution subject to ECS terms of use (see ecsdl.org/site/terms_use) unless CC License in place (see abstract).

$P = 80$ Torr. In most of the depositions α was less than 0.1, which justifies the approximation $\alpha << 1$ made in Eq. [9], and the assumptions made above regarding the monitoring of the total pressure and the flow rate. We found the value of α to be independent of the flow rate, which justifies the assumption of equilibrium conditions at the high temperature reactor under our experimental conditions. Equilibrium at the high temperature reactor may be maintained as long as the flow velocity of the gas through the reactor is slow relative to the length of the silicon column divided by the reaction rate.

As indicated above, the rate-limiting process was found to be the reaction in the high temperature (T_1) zone. It is thus consistent to assume that the deposition rate is proportional to the number of SiF_2 molecules arriving at the deposition reactor per unit time, which is proportional to the value of α times the SiF_4 flow rate. Indeed, as can be seen from Fig. 5, it was found that the deposition rate is linear with the flow rate. In the experiments in which we varied the total pressure and kept the value of $\rho\nu^2$ constant, the flow rate was proportional to $P^{1/2}$ (Eq. [4]) and, since α is proportional to $P^{1/2}$ (Eq. [9]), the deposition rate is expected to be independent of P, as was observed (Fig. 6). From these results we also conclude that under a constant flow velocity (in units of volume per unit time) the deposition rate should increase with the square root of the SiF_4 pressure, and under constant flow rate (in mols per unit time) the deposition rate should vary as the inverse square root of the pressure.

As for the polymerization dynamics, it is recalled that under constant P and ν the temperature (T_1) dependence of $\Delta P/\Delta t$ scaled linearly with the deposition rate. This implies a linear dependence of $\Delta P/\Delta t$ on α, that is, on the partial pressure of SiF_2 in the system. This would be consistent with a monomolecular production mechanism for $(SiF_2)_n$ polymers. On the other hand, from measurements of the dependence of $\Delta P/\Delta t$ on the flow rate and on the total pressure, it was found that $\Delta P/\Delta t$ is proportional to $\rho\nu^2 \cdot P$, which in turn is proportional to $P^2 \cdot \nu^2$ (see Fig. 6 and Eq. [5]). This implies that $\Delta P/\Delta t$ is proportional to $P^{3/2} \cdot \nu^2$ after one takes out the monomolecular reaction dependence on αP. This higher order pressure dependence of $\Delta P/\Delta t$ may imply that the pressure of SiF_4 at the polymerization sites enhances the $(SiF_2)_n$ polymerization rate. The mechanism for the observed pressure and velocity dependence of the polymerization kinetics still remains to be explained.

Film Properties

The optical transmittance and reflectance of the films were measured with Beckman Models ACTA MVII and IR 4250 spectrophotometers. From these measurements the refractive index and the absorption coefficient were derived. Within experimental accuracy these results are identical to previously published results on CVD silicon deposited below 675°C from silane (10).

The optical properties of all films deposited below 675°C were identical. Debye-Scherrer x-ray diffraction analysis of films deposited in another reactor (5) indicated that films deposited between 700° and 900°C are polycrystalline, while below 700°C the films are amorphous, as indicated by the broad diffraction halos and indistinguishable second and third rings in the diffraction patterns. At deposition temperatures between 850° and 900°C a thin yellow powdery deposition was observed. No deposition could be observed above 900°C. The room temperature electrical resistivity of the films deposited below 700°C was $2 \times 10^5\ \Omega \cdot cm$. From photoconductivity measurements a carrier lifetime of the order of 10^{-10} sec is estimated, assuming a mobility of 1 cm^2/V sec. The results of the electrical, optical, and ESR measurements of these films were published elsewhere and they are characteristic of anneal-stable amorphous silicon films (5).

Impurities in the films have been studied by surface electron spectroscopy (Auger and XPS) with a PHI system Model 590A and 555. Depth profiling Auger spectroscopy under Ar^+ sputter etching showed 99.6 ± 4% purity silicon. Oxygen and carbon signals could not be observed within a detectability limit of 0.2 a/o XPS (x-ray photoelectron spectroscopy) confirmed these results regarding oxygen and carbon, but it showed about 0.6 a/o fluorine in the film. The fluorine in the film. The fluorine concentration in the film has been further studied by the nuclear reaction $^{19}F(P,\alpha)^{16}O^*$, as described previously (5). This technique was found to have a resolution of 50 ppm with our counting times. The results showed a concentration between 0.5 and 1.5 a/o fluorine, depending on the substrate temperature during deposition (5). The reason we were not able to detect this fluorine by Auger depth profiling and got smaller values in XPS than with the ion implantation system is probably because the fluorine in the samples is in the form of SiF_4 gaseous molecules which were trapped in the film during deposition. During depth profiling sputter etching these molecules are freed and pumped out of the electron spectrometer, so they could not be detected by the Auger technique which is sensitive only to the composition of the first two or three monolayers of the film. The XPS technique probes at a depth of approximately 20Å, while the nuclear reaction probed the fluorine concentration at a depth of 500Å below the surface, where the SiF_4 molecules can be found. This point has recently been supported by infrared spectroscopy associated with Auger spectroscopy measurements (11). These silicon fluoride molecules were found to be electronically inactive, and there is evidence that when the sample is anneal crystallized at 800°C they leave the film (3, 11).

In summary, we have demonstrated a new deposition method of silicon films from SiF_2 vapor. Deposition temperature can be as low as 550°C with acceptable deposition rates. The properties of the films were found to be similar to the properties of silicon films prepared in the same temperature range by CVD from silane. The transport reaction given by Eq. [1] was studied and the fractional conversion of SiF_4 into SiF_2 at equilibrium at temperatures above 1060°C was deduced. This transport reaction can also be used in conjunction with glow discharge deposition system of fluorinated amorphous silicon (a-Si:F) where the SiF_2 decomposition is assisted by an electric field. This approach is currently being investigated in our laboratory.

Acknowledgments

This research was supported in part by the United States-Israel Binational Science Foundation (BSF), Jerusalem, Israel, and by the Fund for the Promotion of Research at the Technion. The authors acknowledge the efficient technical support of A. Kessel in constructing the deposition system. Our thanks to R. Brener for XPS and Auger analysis, to Prof. R. Kalish for ion implantation services, and to K. Levin for electrical measurements.

Manuscript submitted Dec. 18, 1980; revised manuscript received July 9, 1981.

Any discussion of this paper will appear in a Discussion Section to be published in the June 1982 JOURNAL. All discussions for the June 1982 Discussion Section should be submitted by Feb. 1, 1982.

REFERENCES

1. M. Wolf, Proc. 11th IEEE Photovoltaic Specialists Conference, Phoenix, Arizona (1975).
2. M. Wolf, A. G. MacDiarmid, G. T. Noel, and K.

Downloaded on 2015-06-07 to IP 128.210.126.199 address. Redistribution subject to ECS terms of use (see ecsdl.org/site/terms_use) unless CC License in place (see abstract).

Thallum, in "Proc. 12th IEEE Photovoltaic Specialists Conference" (1976).
3. W. M. Ingle, R. Chaney, and S. Thompson, Motorola Quarterly Reports 2257/1-2257/8, ERDA JPL Contract No. 954442 1976-1978.
4. C. H. Van Dyke, in "The Bond to Halogens and Halogenoids," Part I, A. G. MacDiarmid, Editor, p. 142, Marcel Dekker, Inc., New York (1972).
5. M. Janai, R. Weil, K. H. Levin, B. Pratt, R. Kalish, G. Braunstein, M. Teicher, and M. Wolf, *J. Appl. Phys.*, To be published.
6. W. Braker and A. L. Mossman, "Matheson Gas Data Book," 5th ed., p. 509, Matheson, New Jersey (1971).
7. L. I. Maissel and R. Glang, "Handbook of Thin Film Technology," pp. 11-4 to 11-14, McGraw-Hill Company, New York (1970).
8. See, *e.g.*, "Variable Area Flowmeter Handbook," Vol. 1 (Fischer & Porter Catalog 10A 1021).
9. C. C. Pease, U.S. Pat. 2,840,588 (1958).
10. M. Janai, D. D. Allred, D. C. Booth, and B. O. Seraphin, *Solar Energy Mater.*, **1**, 11 (1979).
11. C. J. Fang, L. Hey, H. R. Shanks, K. J. Grutz, and M. Cardona, *Phys. Rev. B.*, To be published.

Electronic Characterization of Heteroepitaxial Silicon-on-Sapphire by Surface Photovoltage Spectroscopy

J. Lagowski*

Massachusetts Institute of Technology, Cambridge, Massachusetts 02139

and L. Jastrzebski* and G. W. Cullen*

RCA Laboratories, Princeton, New Jersey 08540

ABSTRACT

Surface photovoltage spectroscopy was successfully applied to silicon-on-sapphire and it enables simultaneous determination of band structure, trapping centers, deep levels, the refractive index, and the film thickness. Studies of "as-grown" and ion-implanted films revealed a noticeable degree of amorphization manifested by 1.45 eV energy gap structure clearly resolved in addition to standard 1.1 eV structure of bulk Si. Three deep levels were identified, *i.e.*, electron trap at $E_c - E_t = 0.25$ eV, hole trap at $E_t - E_v = 0.15$ eV, and deep centers at $E_c - E_t = 0.6$ eV. It has been found that the degree of amorphization and concentration of deep centers in the layers depends on the thermal history of the SOS film.

Rapidly growing need for high speed, radiation resistance CMOS memories and microprocessors with large capacity and high packing density puts new demands on SOS technology. One of the factors which can limit circuit performance is the presence of deep levels in the silicon-on-sapphire. Deep levels acting as traps can decrease speed, shift threshold voltage, and/or cause excessive junction leakage of transistors in the circuit. A nonuniform distribution of deep centers across a wafer can result in nonuniform yield and circuit performance on the wafer. These facts emphasize the importance of developing methods to experimentally assess the sources of deep centers in as-grown layers and processed silicon films.

Techniques for the characterization of heteroepitaxial silicon have been reviewed by Ham (1). Most of these methods rely on the measurement of test structures on processed wafers or on resistivity and capacitance measurements on as-grown films. Recently a u.v. reflectance method has been developed which allows quantitative characterization of the crystallinity in SOS films (2). These techniques have been designed as effective and practical tools for establishing screening criteria to inspect the quality of as-grown wafers used for fabrication of device structures. They do not provide direct information about deep levels in SOS films.

Previous studies of polycrystalline and amorphous silicon and of dislocation structures in elemental semiconductors have demonstrated the promising character of photoelectric measurements in assessing the electronic and optical properties of silicon, and in identifying the mechanisms of phenomena related to defects and disorder (3-5). The photovoltage spectroscopy technique selected for the present study is rather specific among photoelectric effects as it permits the measurement of bulk material as well as the conducting or high resistivity films on insulating or metallic substrates (6-8). Furthermore, this technique does not require ohmic contacts, and if necessary it can be utilized in a nondestructive, contactless, configuration employing capacitive coupling to the sample. Therefore, as-grown wafers and wafers after different processing steps can be analyzed without the fabrication of test structures. Also a light spot can be easily focused to a small area which permits the characterization of defect distribution on a microscale.

This investigation has been undertaken to assess the feasibility of using photovoltage measurements for characterization of defects in SOS. Information concerning the deep states (their energy levels and relaxation time) and the basic parameters of SOS layers (the band structure, the film thickness, and the refractive index) were obtained from the spectral, transient, and temperature dependence of the photovoltage. The measurements performed on layers after different stages of processing (as-grown, ion-implanted, and heat-treated) show that the photovoltage technique is able to detect a variety of defect structures in SOS films.

Experimental

In the present study the photovoltage generated by a monochromatic light (energy range 0.5-3.5 eV) was measured with respect to a semitransparent gold electrode separated from the SOS film by a 10 μm thick Myler foil (MIS configuration) or directly evaporated on SOS film (MS configuration).

* Electrochemical Society Active Member.
Key words: defects, amorphous, silicon-on-sapphire, surface photovoltage.

Downloaded on 2015-06-07 to IP 128.210.126.199 address. Redistribution subject to ECS terms of use (see ecsdl.org/site/terms_use) unless CC License in place (see abstract).